

New Design Procedure to Determine the Taper Transition for Impedance Matching Between Microstrip Line and SIW Component

Ricardo Caranicola Caleffo

*Department of Electronic Systems Engineering
Polytechnic School, University of São Paulo (USP)
Av. Prof. Luciano Gualberto, Trav. 3, nº 380, SP - São Paulo, Brazil
ricardocaleffo@usp.br*

Abstract— Normally the physical dimensions of the taper transition that realizes the impedance matching between the impedance of the feeding line built in microstrip line technology and the impedance of the component built in Substrate Integrated Waveguide (SIW) technology are obtained by computational optimization processes due the difficulty of analytical treatment. This research work presents a new empirical approach to determine all the physical dimensions of this particular planar transition without using any computational optimization process. The well-defined design procedure is based on an approximation according with electromagnetic simulations and electromagnetic theory. The main goal is to facilitate the integration between SIW technology and planar circuits. The whole design procedure considers central frequency for the recommended bandwidth in the TE_{10} propagation mode and power-voltage impedance definition for the SIW. Two structures are designed on RT/duroid 5880 to operate in the X band and Ku band, and the frequency response for both structures are compared by electromagnetic simulation and experimental results. The structure operating in X Band demonstrated return loss better than 10.0 dB at 61.67% of the considered bandwidth and the structure operating in Ku Band demonstrated return loss better than 10.0 dB at 72.88% of the considered bandwidth.

Index Terms— Planar circuits, SIW technology, Taper transitions.

I. INTRODUCTION

Rectangular Waveguides (RWG) are widely applied in the microwave frequencies due a low power dissipation and high quality factor. In contrast, shows as disadvantage a high fabrication cost and the integration with planar circuits require sophisticated transitions. To avoid these problems, has been proposed a structure called Substrate Integrated Waveguide (SIW). The components built using SIW technology are designed and fabricated on a planar dielectric substrate low losses and having periodical metalized vias that replaces the side walls of the traditional RWG, confining the electromagnetic wave inside the dielectric substrate, allowing in this way an easy integration with planar circuits [1]. The SIW technology can be employed in applications to operate since the S band until Ka band. The frequency limitation in SIW technology occurs due the dielectric loss affects strongly the electromagnetic wave propagation. Fig. 1 shows a generic SIW.

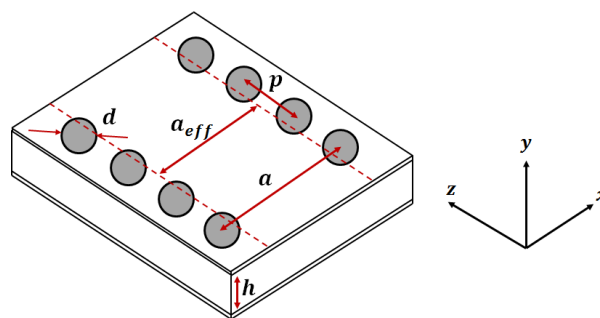


Fig. 1. Generic substrate integrated waveguide.

Where a_{eff} is the effective width, h is the dielectric substrate thickness, d is the diameter of metalized vias, p is the periodical spacing between two consecutives metalized vias, and a is the spacing between the two rows of metalized vias. Due the side walls are replaced by metalized vias, the longitudinal electrical current is not allowed, so the SIW support just the TE propagation mode [1], [2]. The absence of TM propagation mode creates a favorable condition for design bandpass filters [1], [3]. The electromagnetic waves propagation in SIW technology is affected by the insertion of periodical metalized vias and some studies and analyses has been done for understanding the operation of this technology [4], [5]. Due the difference of propagation modes and guided modes, modeling of conductor, dielectric, and radiation losses in SIW technology is also a target of study [6]. The SIW technology can be applied in many applications, such as traditional structures of power dividers/combiners [7] and dividers/combiners based on directional couplers [8], [9]. Normally the components built in SIW technology are fed by a microstrip line with a characteristic impedance of 50Ω and the integration between them can be made by a taper transition, such as [7]-[9]. The taper transition realizes the impedance matching between the impedance of the feeding line and the impedance of the SIW component. Due the difficult of analytical treatment, computational optimization processes has been widely used to determine the physical dimensions of this planar transition. There are some studies that provide an appropriate treatment for analyze the taper transition and some examples have been demonstrated [10], [11].

This research work presents a new empirical approach to determine all the physical dimensions of the taper transition in an easy way without using any computational optimization process. The main aim is to obtain return loss better than 10.0 dB and low insertion loss in the recommended bandwidth for the SIW. The paper is organized according with the next description: Section II presents the main design considerations for the SIW component and the main characteristics for the feeding line. Section III presents the well-defined design procedure based on an approximation according with electromagnetic simulations and electromagnetic theory to determine the physical dimensions of the taper transition. Section IV presents two application examples using the design procedure established in this paper in the X band and Ku band. Both application examples consider TE_{10} propagation mode and are designed and fabricated on a RT/duroid 5880. Finally the Section V shows the main comments and conclusions obtained in this research work.

II. DESIGN CONSIDERATIONS

An important design factor is know how the impedance of each element of the whole structure operate as a function of frequency to realize the impedance matching between the impedance of the feeding line and the impedance of the SIW component. The dielectric substrate loss is also an important design factor and the $\tan\delta$ must be as low as possible. The dielectric substrate thickness provides the height of the SIW component and the feeding line, being in this way, the only design parameter that does not allow changes after the choice of the dielectric substrate.

A. Substrate Integrated Waveguide

The RWG concepts and theory can be directly applied in studies and projects involving SIW technology. Generally the component built in SIW technology operates in TE_{10} mode and higher modes are not considered due the undesirable electric field configuration. But is necessary knowing the operation frequency of TE_{20} propagation mode to avoid the SIW component operates in this particular propagation mode. The cutoff frequencies for the SIW are written as a function of the effective widths [1].

$$f_{c_{TE_{m0}SIW}} = \frac{c}{2\sqrt{\epsilon_r}} \left(\frac{m}{a_{eff_{m0}}} \right) \quad (1)$$

Where $m \geq 1$, ϵ_r is the relative dielectric constant, and c is the speed of light. According with [1], [2] the equations of the cutoff frequencies for the TE_{10} and TE_{20} propagation modes are given by (2)-(3).

$$f_{c_{TE_{10}SIW}} = \frac{c}{2\sqrt{\epsilon_r}} \left(\frac{1}{a_{eff_{10}}} \right) = \frac{c}{2\sqrt{\epsilon_r}} \left(a - 1.08 \frac{d^2}{p} + 0.1 \frac{d^2}{a} \right)^{-1} \quad (2)$$

$$f_{c_{TE_{20}SIW}} = \frac{c}{2\sqrt{\epsilon_r}} \left(\frac{2}{a_{eff_{20}}} \right) = \frac{c}{\sqrt{\epsilon_r}} \left(a - \frac{d^2}{1.1p} + 0.1 \frac{d^3}{6.6p^2} \right)^{-1} \quad (3)$$

The parameters a , p , and d determine the effective widths for the TE_{10} and TE_{20} propagation modes, which these determine the cutoff frequencies. The choice for these three parameters is not random and depends on four rules for the SIW operate as a waveguide [1]. After determine the cutoff frequencies for the TE_{10} and TE_{20} propagation modes, it is possible determine a bandwidth for the component built in SIW technology. According with the recommended bandwidth for the RWG [12], the recommended bandwidth for the SIW that guarantees the operation exactly in the TE_{10} propagation mode and low losses is given by (4).

$$1.25 \cdot f_{c_{TE_{10}SIW}} < f < 0.95 \cdot f_{c_{TE_{20}SIW}} \quad (4)$$

The central frequency of the recommended bandwidth given by (4) can be written by (5).

$$f_o = \frac{1.25 \cdot f_{c_{TE_{10}SIW}} + 0.95 \cdot f_{c_{TE_{20}SIW}}}{2} \quad (5)$$

With the recommended bandwidth (4) and central frequency (5) obtained it is possible evaluate the cross-section impedance of the SIW component in the TE_{10} propagation mode. The cross-section impedance of the SIW component can be defined considering three different impedance definitions.

This research work employs the power-voltage (P-V) impedance definition due the majority of electromagnetic simulators using this impedance definition. The power-voltage (P-V) impedance definition can be written by (6),

$$Z_{SIW(P-V)} = \frac{V \cdot V^*}{P} \quad (6)$$

where V is the voltage drop between the top and the bottom metallic walls of the SIW component, V^* is the conjugated of V , and P is the incident power at the cross-section of the SIW component given by the Poynting theorem. For the TE_{10} propagation mode, the cross-section impedance can be written according with the SIW physical dimensions in the same way as given by the RWG [1], [12],

$$Z_{SIW(P-V)} = \frac{2h}{a_{eff10}} \frac{\eta_0}{\sqrt{\epsilon_r}} \left[1 - \left(\frac{f_c}{f} \right)^2 \right]^{\frac{1}{2}} \quad (7)$$

where h is the dielectric substrate thickness, a_{eff10} is the effective width for the TE_{10} propagation mode, η_0 is the intrinsic impedance of the free space, ϵ_r is the relative dielectric constant of the substrate, f_c is the cutoff frequency, and f is the operation frequency. At the central frequency of the recommended bandwidth for TE_{10} propagation mode (5), the cross-section impedance of the SIW component can be expressed by (8).

$$Z_{SIW(P-V)} = \frac{2h}{a_{eff10}} \frac{\eta}{\sqrt{\epsilon_r}} \left[1 - \left(\frac{2f_{cTE_{10}SIW}}{1.25f_{cTE_{10}SIW} + 0.95f_{cTE_{20}SIW}} \right)^2 \right]^{\frac{1}{2}} \quad (8)$$

B. Feeding line

The feeding line used in this work is built in microstrip line technology and has 50Ω of impedance characteristic and it is designed at the central frequency of the recommended bandwidth by (5).

III. DESIGN PROCEDURE FOR TAPER TRANSITION

The Fig. 2 shows a symmetric structure used in this research work containing two microstrip lines that feeds the whole structure with same physical dimensions, a substrate integrated waveguide, and two taper transitions that realizes the impedance matching with same physical dimensions.

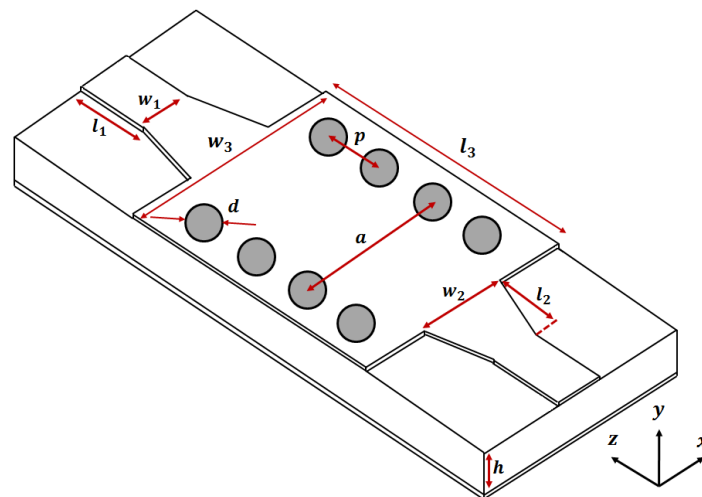


Fig. 2. Complete structure used in this research work.

The taper transition in Fig. 2 is responsible to realize the impedance matching between the impedance of the feeding line and the impedance of the SIW component. The Fig. 3 shows a schematic of impedance matching considered in this research work.

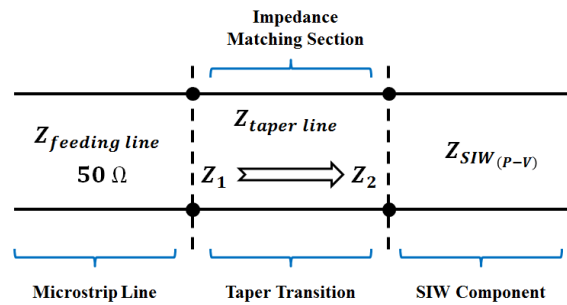


Fig. 3. Schematic of impedance matching between feeding line and SIW component.

The cross-section impedance between the feeding line and the taper transition is defined as $Z_1 = 50 \Omega$ and the cross-section impedance between the taper transition and the SIW component is defined as Z_2 . For a good impedance matching Z_2 must be closest possible of $Z_{SIW(p-v)}$. The Z_2 impedance value is given by the microstrip line impedance [13], where the cross-section physical dimensions are given by w_2 and h . For this work is valid the relation $w_2/h > 1$.

$$Z_2 = \frac{120\pi}{\sqrt{\epsilon_{e2}} \left\{ \left(\frac{w_2}{h} \right) + 1.393 + 0.667 \cdot \ln \left[\left(\frac{w_2}{h} \right) + 1.444 \right] \right\}} \quad (9)$$

where ϵ_{e2} is the effective dielectric constant for a microstrip line with physical dimensions w_2 and h [13].

The physical dimension l_2 also makes a contribution for the impedance matching. According with [14], the reflection coefficient for a triangular taper is a function of l_2 .

$$\Gamma(\theta) = \left| \frac{1}{2} \ln \left(\frac{Z_2}{Z_1} \right) \left[\frac{\sin(\beta l_2/2)}{\beta l_2/2} \right]^2 \right| e^{-j\beta l_2} \quad (10)$$

where β is the propagation constant of the tapered line [14].

In many cases, the taper transition physical dimensions are obtained by computational optimization processes due the difficult of an analytical treatment. One of the factors that increase the difficulty of analytical treatment is the difference of field configuration between SIW component and microstrip line. The substrate integrated waveguide support just TE propagation mode [1], [2] and the microstrip line technology in many practical applications has a quasi-TEM propagation mode [13].

According with Fig. 2, the taper transition physical dimensions are given by w_1 , w_2 , and l_2 , whence the physical dimension w_1 is given by the feeding line. Therefore, the physical dimensions w_2 and l_2 are the dimensions to be determined. In this section will be demonstrated a new empirical approach for determine these two physical dimensions.

The taper transition is a microstrip line with variable width, beginning with a width w_1 and finishing with a width w_2 , therefore, an effective dielectric constant value cannot be applied directly in the same way as is defined for a simple microstrip line.

This research work will approximate an effective dielectric constant value for the taper transition and this respective approximated value has the same effective dielectric constant value of the feeding line. This approximation considers the electromagnetic wave that is being propagated along the taper transition has the same wavelength of the electromagnetic wave that is being propagated along the feeding line. The proposed approximation is done due initially the only available physical dimension for the taper transition is w_1 , given by the feeding line width.

To justify this approximation was designed, optimized, and simulated 13 structures in six different operation bands using the High Frequency Structure Simulator (HFSS). For each structure was obtained a return loss better than 10.0 dB in the recommended bandwidth by (4). The main aim of the 3D computational electromagnetic simulations realized is to verify how much the difference between the widths w_1 and w_2 affects the effective dielectric constant value and the Z_2 impedance value.

Will be shown that a mean error lower than 6% is present when is taken a unique effective dielectric constant value for the taper transition and feeding line, and a mean error lower than 7% is present in the impedance matching between the taper transition and the SIW component considering the proposed approximation.

The reference values used for the proposed approximation are $\sqrt{\epsilon_{e1}}$ and $\sqrt{\epsilon_{e2}}$, where the first one considers the width w_1 and the second one considers the width w_2 , and both of them have the same dielectric substrate thickness (h). The reason for considerer $\sqrt{\epsilon_e}$ is due the wavelength calculation be divided by this term and all the physical dimensions considered are a function of the wavelength.

A smaller difference between $\sqrt{\epsilon_{e1}}$ and $\sqrt{\epsilon_{e2}}$ provides a better approximation for a unique effective dielectric constant value (ϵ_{e1}), where $\sqrt{\epsilon_{e1}}$ it is the error reference for the proposed approximation. To obtain the error for the proposed approximation (11) it is considered.

$$Error(\sqrt{\epsilon_e})_{\%} = \frac{|\sqrt{\epsilon_{e2}} - \sqrt{\epsilon_{e1}}|}{\sqrt{\epsilon_{e1}}} \cdot 100 \quad (11)$$

Table I shows the 13 structures designed and optimized covering since S band until Ka band, and considers the bandwidth given by (4) and central frequency given by (5). The structures shown in Table I have two different values of dielectric substrate thickness, 0.51 mm and 0.63 mm. The substrate integrated waveguide and feeding lines physical dimensions were obtained according with the design considerations presented in Section II. The taper transition physical dimensions w_2 and l_2 were obtained by computational optimization processes providing a return loss better than 10.0 dB and low insertion loss in the considered bandwidth.

Table I. 13 structures designed and optimized covering since S band until Ka band.

Simulation	1	2	3	4	5	6	7	8	9	10	11	12	13
Band	S	S	S	C	C	C	X	X	X	X	Ku	K	Ka
ϵ_r	2.20	8.20	10.20	2.20	8.20	10.20	2.20	2.33	4.40	6.15	2.20	2.20	2.20
$\tan\delta (10^{-3})$	0.90	2.00	2.30	0.90	2.00	2.30	0.90	1.20	2.00	0.90	0.90	0.90	0.90
$f_{cTE_{10SIW}}$ (GHz)	1.73	1.73	1.73	4.00	4.00	4.00	6.56	6.56	6.56	6.56	9.74	14.34	20.80
f_o (GHz)	2.72	2.72	2.72	6.30	6.30	6.30	10.31	10.31	10.31	10.31	14.91	22.60	32.76
h (mm)	0.51	0.63	0.63	0.51	0.63	0.63	0.51	0.51	0.63	0.63	0.51	0.51	0.51
l_1 (mm)	20.10	11.76	10.60	8.68	5.00	4.51	5.20	5.20	3.95	3.42	3.58	2.38	1.65
w_1 (mm)	1.57	0.71	0.57	1.54	0.71	0.60	1.55	1.49	1.23	0.93	1.55	1.58	1.63
a (mm)	60.24	31.40	27.12	26.05	13.88	12.50	15.83	15.83	11.66	9.81	11.40	7.59	5.24
p (mm)	2.40	4.00	5.08	2.00	2.00	2.00	2.54	2.54	2.00	1.80	1.50	1.20	1.00
d (mm)	1.20	2.00	1.00	1.20	1.20	1.20	1.00	1.00	1.20	1.00	1.00	0.64	0.60
l_3 (mm)	74.00	61.00	58.00	40.00	40.00	40.00	45.00	45.00	40.00	40.00	27.00	20.30	20.00
w_3 (mm)	58.00	45.00	30.00	34.00	22.00	22.00	18.00	18.00	20.00	22.00	16.00	15.00	12.00
l_2 (mm)	27.20	15.00	13.90	11.60	6.60	6.00	7.09	7.10	5.40	4.50	4.90	3.30	2.20
w_2 (mm)	12.60	7.50	5.30	6.50	3.35	2.60	3.43	3.60	2.75	2.30	3.10	1.50	1.20
l_2/w_2	2.16	2.00	2.62	1.79	1.97	2.31	2.07	1.97	1.96	1.96	1.58	2.20	1.83

According with Table I an arithmetic mean considering the 13 relations l_2/w_2 can be written.

$$\frac{l_2}{w_{2mean}} = \sum_{i=1}^{13} \left(\frac{l_{2i}}{w_{2i}} \right) / 13 = 2.03 \quad (12)$$

And an approximation can be written by (13) according with (12).

$$\frac{l_2}{w_{2mean}} = 2 \quad (13)$$

According with (8) and (9), the impedance values for the 13 structures are shown in Table II.

Table II. Impedance values for the 13 structures.

Simulation	1	2	3	4	5	6	7	8	9	10	11	12	13
$Z_1 (\Omega)$	50.00	50.00	50.00	50.00	50.00	50.00	50.00	50.00	50.00	50.00	50.00	50.00	50.00
$Z_2(\Omega)$	8.86	9.02	11.02	16.43	18.20	20.12	28.72	27.10	29.64	29.14	31.92	55.11	64.13
$Z_{SIW(p-v)} (\Omega)$	5.70	7.13	7.13	13.22	16.52	16.53	21.72	21.71	27.14	27.14	29.45	47.73	69.05

According with Table II the Z_2 impedance values are tending to $Z_{SIW(p-v)}$ impedance values, demonstrating in this way, the impedance matching provided by the taper transition.

Table III shows the error for the proposed approximation in this research work considering the 13 designed and optimized structures. To obtain the value for ϵ_{e_1} was considered the physical dimensions h and w_1 and for ϵ_{e_2} was considered the physical dimensions h and w_2 . The error considers (11).

Table III. Error for the proposed approximation in this research work considering the 13 designed and optimized structures.

Simulation	1	2	3	4	5	6	7	8	9	10	11	12	13
ϵ_{e_1}	1.87	5.65	6.81	1.87	5.65	6.84	1.87	1.96	3.33	4.42	1.87	1.87	1.88
ϵ_{e_2}	2.09	7.14	8.55	2.03	6.59	7.92	1.96	2.07	3.58	4.82	1.95	1.87	1.84
$Error(\sqrt{\epsilon_e})\%$	5.74	12.37	12.00	4.23	7.98	7.59	2.38	2.78	3.56	4.32	2.07	0.15	0.87

According with Table III an arithmetic mean for the error can be written conform (14).

$$Error(\sqrt{\varepsilon_e})_{\%mean} = \sum_{i=1}^{13} \left(\frac{|\sqrt{\varepsilon_{e2_i}} - \sqrt{\varepsilon_{e1_i}}|}{\sqrt{\varepsilon_{e1_i}}} \cdot 100 \right) / 13 = 5.08\% \quad (14)$$

According with (14) a mean error lower than 6% is present in this proposed approximation considering the 13 designed and optimized structures. Due the low mean error obtained, a unique effective dielectric constant value is taken for the taper transition and feeding line (ε_{e1}). Therefore, the wavelength of an electromagnetic wave that is being propagated along the taper transition is approximated to the wavelength of an electromagnetic wave that is propagated along the feeding line with a mean error lower than 6%. The obtained error is related with 13 designed and optimized structures in Table I.

Considering the proposed approximation, an impedance Z_2 can be rewrite considering $\sqrt{\varepsilon_{e1}}$.

$$Z_2(\sqrt{\varepsilon_{e1}}) = \frac{120\pi}{\sqrt{\varepsilon_{e1}} \left\{ \left(\frac{w_2}{h} \right) + 1.393 + 0.667 \cdot \ln \left[\left(\frac{w_2}{h} \right) + 1.444 \right] \right\}} \quad (15)$$

To evaluate the impact of the proposed approximation in the impedance matching between the taper transition and the SIW component, a mean error can be obtained for the impedance matching. For the error related with the impedance matching, the $Z_2(\sqrt{\varepsilon_{e2}})$ impedance value is taken as reference.

$$Error[Z_2(\sqrt{\varepsilon_e})]_{\%} = \frac{|Z_2(\sqrt{\varepsilon_{e1}}) - Z_2(\sqrt{\varepsilon_{e2}})|}{Z_2(\sqrt{\varepsilon_{e2}})} \cdot 100 \quad (16)$$

Table IV shows a comparison between $Z_2(\sqrt{\varepsilon_{e1}})$ and $Z_2(\sqrt{\varepsilon_{e2}})$, the Z_1 and $Z_{SIW(p-v)}$ impedance values are also considered. The main aim of this comparison shown in Table IV is to evaluate the difference in the impedance matching when is considered a unique effective dielectric constant value.

Table IV. Impedance values for the 13 structures considering the proposed approximation and the error caused by it.

Simulation	1	2	3	4	5	6	7	8	9	10	11	12	13
$Z_1(\Omega)$	50.00	50.00	50.00	50.00	50.00	50.00	50.00	50.00	50.00	50.00	50.00	50.00	50.00
$Z_2(\sqrt{\varepsilon_{e1}}) (\Omega)$	9.71	10.62	12.83	17.28	19.98	21.74	28.87	27.18	29.95	29.39	31.17	51.66	59.24
$Z_2(\sqrt{\varepsilon_{e2}}) (\Omega)$	8.86	9.02	11.02	16.43	18.20	20.12	28.72	27.10	29.64	29.14	31.92	55.11	64.13
$Error[Z_2(\sqrt{\varepsilon_e})]_{\%}$	9.59	17.74	16.42	5.17	9.78	8.05	0.52	0.30	1.05	0.86	2.35	6.26	7.63
$Z_{SIW(p-v)}(\Omega)$	5.70	7.13	7.13	13.22	16.52	16.53	21.72	21.71	27.14	27.14	29.45	47.73	69.05

According with Table IV, an arithmetic mean for the impedance matching error considering the 13 impedance values for $Z_2(\sqrt{\varepsilon_{e1}})$ and $Z_2(\sqrt{\varepsilon_{e2}})$ can be written by (17).

$$Error[Z_2(\sqrt{\varepsilon_e})]_{\%mean} = \sum_{i=1}^{13} \left(\frac{|Z_2(\sqrt{\varepsilon_{e1}})_i - Z_2(\sqrt{\varepsilon_{e2}})_i|}{Z_2(\sqrt{\varepsilon_{e2}})_i} \cdot 100 \right) / 13 = 6.60\% \quad (17)$$

According with (17), the proposed approximation affects less than 7% the impedance matching between the taper transition and the SIW component.

Based on the proposed approximation, a wavelength of an electromagnetic wave being propagated along the taper transition can be calculated considering central frequency at the recommended band by (5) and the effective dielectric constant of the feeding line.

$$\lambda_{taper}(\sqrt{\varepsilon_{e_1}}, f_o) = \frac{2c}{(1.25 \cdot f_{c10SIW} + 0.95 \cdot f_{c20SIW}) \cdot \sqrt{\varepsilon_{e_1}}} \quad (18)$$

Table V shows a comparison between the wavelength λ_{taper} and the physical dimension l_2 related with the 13 designed structures in Table I. The main aim of this comparison is to obtain a relation between the wavelength λ_{taper} and the physical dimension l_2 .

Table V. Comparison between approximated taper wavelength (λ) and the taper length.

Simulation	1	2	3	4	5	6	7	8	9	10	11	12	13
ε_{e_1}	1.87	5.65	6.81	1.87	5.65	6.84	1.87	1.96	3.33	4.42	1.87	1.87	1.88
f_o (GHz)	2.72	2.72	2.72	6.30	6.30	6.30	10.31	10.31	10.31	10.31	14.91	22.6	32.76
λ_{taper} (mm)	80.62	46.40	42.25	34.83	20.03	18.20	21.28	20.79	15.94	13.83	14.71	9.70	6.69
l_2 (mm)	27.20	15.00	13.90	11.60	6.60	6.00	7.09	7.10	5.40	4.50	4.90	3.30	2.20
λ_{taper}/l_2	2.96	3.09	3.04	3.00	3.04	3.03	3.00	2.93	2.95	3.07	3.00	2.94	3.04

According with Table V, an arithmetic mean relation λ_{taper}/l_2 can be written.

$$\frac{\lambda_{taper}(\sqrt{\varepsilon_{e_1}}, f_o)}{l_2}_{mean} = \sum_{i=1}^{13} \left[\frac{\lambda_{taper}(\sqrt{\varepsilon_{e_1}}, f_o)_i}{l_{2i}} \right] / 13 = 3.01 \quad (19)$$

An approximation can be written by (20) according with (19).

$$\frac{\lambda_{taper}(\sqrt{\varepsilon_{e_1}}, f_o)}{l_2}_{mean} = 3 \quad (20)$$

Therefore, according with (18) and (20) an equation for the physical dimension l_2 can be written.

$$l_2 = \frac{2c}{3 \cdot (1.25 \cdot f_{c10SIW} + 0.95 \cdot f_{c20SIW}) \cdot \sqrt{\varepsilon_{e_1}}} \quad (21)$$

And according with (13) and (21) an equation for the physical dimension w_2 can be written.

$$w_2 = \frac{c}{3 \cdot (1.25 \cdot f_{c10SIW} + 0.95 \cdot f_{c20SIW}) \cdot \sqrt{\varepsilon_{e_1}}} \quad (22)$$

Both equations obtained in this research work can be directly applied to determine in an easy way the physical dimensions l_2 and w_2 of the taper transition, providing the impedance matching between the impedance of the feeding line and the impedance of the SIW component. Of course that the obtained equations are not exact but were proposed considering low mean error for the effective dielectric constant value and impedance matching between the taper transition and SIW component. The empirical design procedure developed in this paper is applied in two application examples to validate (21) and (22). Section IV presents the application examples.

IV. APPLICATION EXAMPLES OF THE DESIGN PROCEDURE DEVELOPED

This section presents two application examples using the design procedure developed in Section III to demonstrate the validity of (21) and (22). According with Section II, the characteristic impedance of the feeding line is 50Ω for both structures. The first example considers the X band and the second example considers the Ku band. All physical dimensions follow the schematic of Fig. 2. The l_3 lengths of both designed and fabricated structures were defined considering at least one guide wavelength, which this was calculated considering (5) and the w_3 widths are at least 25% larger than

the a widths to not affect the mechanical rigidity of the SIW. The via cylinders of both structures were mechanically drilled and are metalized. Both structures have a rigid cooper plate soldered under the ground plane to avoid mechanical deformation due the high flexibility of the chosen substrate. The cooper plate does not affect the results and improve the mechanical rigidity. Both application examples were simulated in the HFSS and the experimental results were obtained with a Hewlett Packard 8722D Network Analyzer, 50 MHz – 40 GHz. The simulation results are represented by black dashed lines and experimental results by black solid lines. The gray area shows the recommended bandwidth.

A. Application example considering X Band

This application example is designed on RT/duroid 5880. According with Section II, the feeding line and substrate integrated waveguide physical dimensions are shown in Table VI.

Table VI. Feeding line and SIW physical dimensions for application example in X Band.

h (mm)	w_1 (mm)	l_1 (mm)	a (mm)	d (mm)	p (mm)	w_3 (mm)	l_3 (mm)
0.51	1.55	5.20	15.98	1.00	1.90	20.00	44.00

According with the physical dimensions in Table VI, the SIW component operates in a bandwidth given by (4) and central frequency is given by (5).

$$8.20 < f < 12.47 \text{ (GHz)}$$

$$f_o = 10.33 \text{ GHz}$$

According with the proposed approximation in this research work, the effective dielectric constant for the feeding line and taper transition is

$$\epsilon_{e_1} = 1.87$$

The central frequency and the effective dielectric constant can be used in (21) and (22) to obtain the taper transition physical dimensions, as shown in Table VII.

Table VII. Taper transition physical dimensions for application example in X Band.

h (mm)	w_1 (mm)	w_2 (mm)	l_2 (mm)
0.508	1.55	3.54	7.08

With $\sqrt{\epsilon_{e_1}}$ and all the physical dimensions obtained, the impedance values, and the reflection coefficient calculated considering central frequency of 10.33 GHz can be written in Table VIII.

Table VIII. Impedance values and reflection coefficient for the application example in X Band.

Z_1 (Ω)	$Z_2(\sqrt{\epsilon_{e_1}})$ (Ω)	$Z_{SIW(p-v)}$ (Ω)	$\Gamma(\theta)$	$ \Gamma(\theta) $ (dB)
50.00	28.26	21.70	$0.24e^{-j\frac{2\pi}{3}}$	12.40

Figure 4 shows the structure built to operate in X Band.

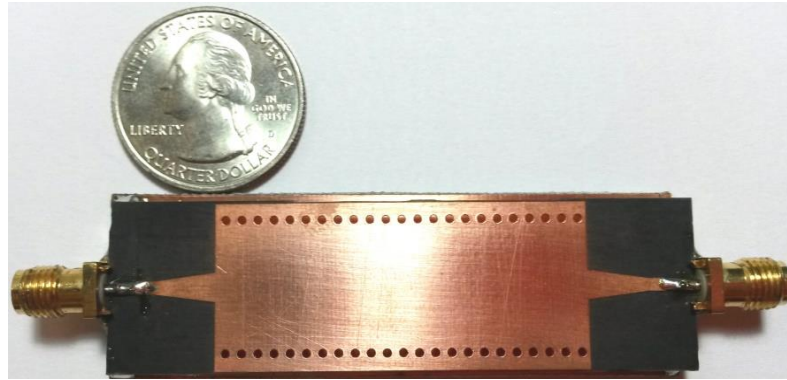


Fig. 4 Structure built to operate in X Band.

The measurement setup for the structure operating in X Band is shown in Fig. 5.

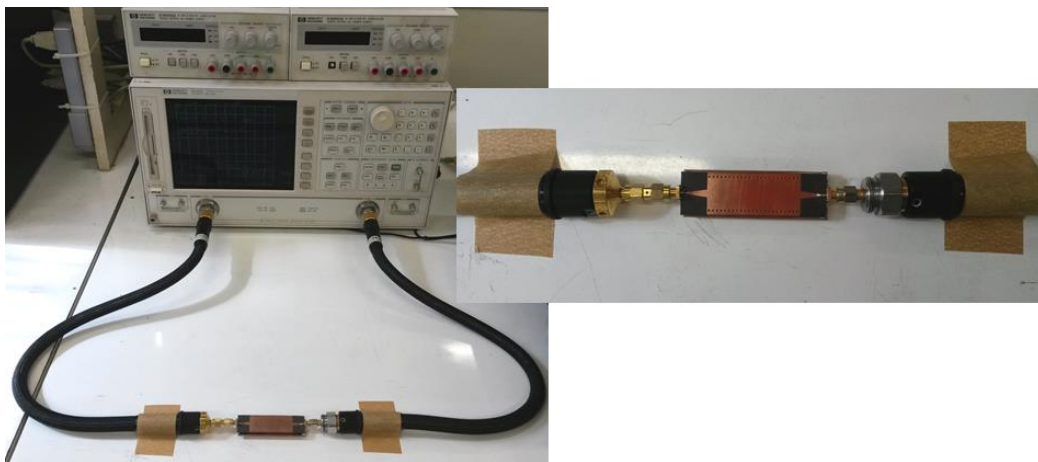


Fig. 5 Structure built to operate in X Band.

The simulated and measured S parameters obtained for the structure operating in X band are shown in Fig. 6.

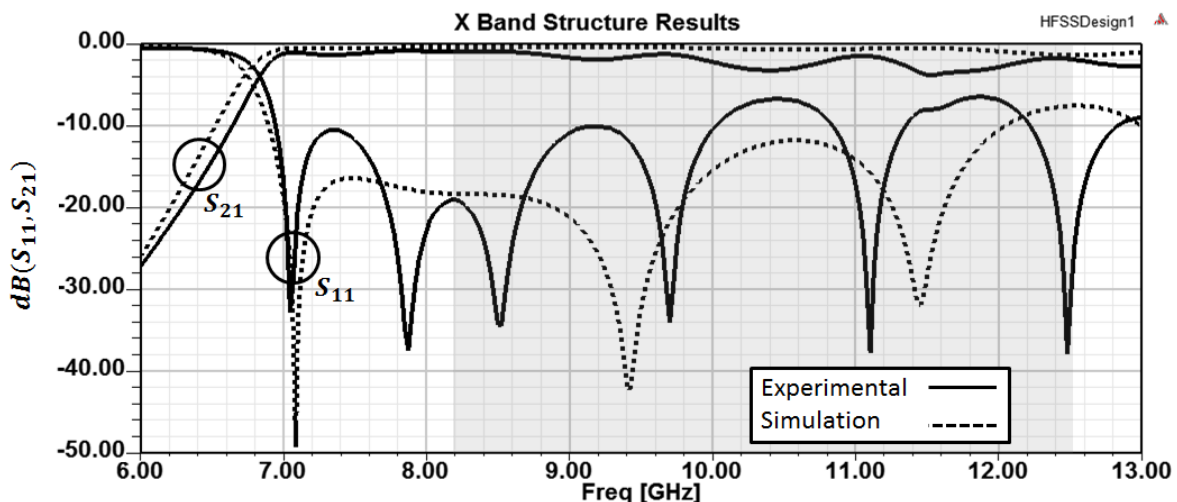


Fig. 6 S parameters obtained for the structure built to operate in X Band.

The simulation results indicated return losses better than 10.0 dB in almost the whole recommend bandwidth. The experimental results presented some degradation in comparison with the simulated ones. The calculated value of the reflection coefficient is -12.40 dB, which this match with the electromagnetic simulation, but the experimental results shows a reflection of -7.0 dB.

B. Application example considering Ku Band

This application example is designed on RT/duroid 5880. According with Section II, the feeding line and substrate integrated waveguide physical dimensions are shown in Table IX.

Table IX. Feeding line and SIW physical dimensions for application example in Ku Band.

h (mm)	w_1 (mm)	l_1 (mm)	a (mm)	d (mm)	p (mm)	w_3 (mm)	l_3 (mm)
0.51	1.55	3.58	11.44	1.00	1.50	16.00	27.00

According with the physical dimensions in Table IX, the SIW component operates in a bandwidth given by (4) and central frequency is given by (5).

$$11.77 < f < 17.73 \text{ (GHz)}$$

$$f_o = 14.75 \text{ GHz}$$

According with the proposed approximation in this research work, the effective dielectric constant for the feeding line and taper transition is

$$\epsilon_{e_1} = 1.87$$

The central frequency and the effective dielectric constant can be used in (21) and (22) to obtain the taper transition physical dimensions, as shown in Table X.

Table X. Taper transition physical dimensions for application example in Ku Band.

h (mm)	w_1 (mm)	w_2 (mm)	l_2 (mm)
0.51	1.55	2.48	4.96

With $\sqrt{\epsilon_{e_1}}$ and all the physical dimensions obtained, the impedance values, and the reflection coefficient calculated considering central frequency of 14.75 GHz can be written Table XI.

Table XI. Impedance values and reflection coefficient for the application example in Ku Band.

Z_1 (Ω)	$Z_2(\sqrt{\epsilon_{e_1}})$ (Ω)	$Z_{SIW(p-v)}$ (Ω)	$\Gamma(\theta)$	$ \Gamma(\theta) $ (dB)
50.00	36.85	31.40	$0.13e^{-j\frac{2\pi}{3}}$	17.72

Figure 7 shows the structure built to operate in Ku Band.

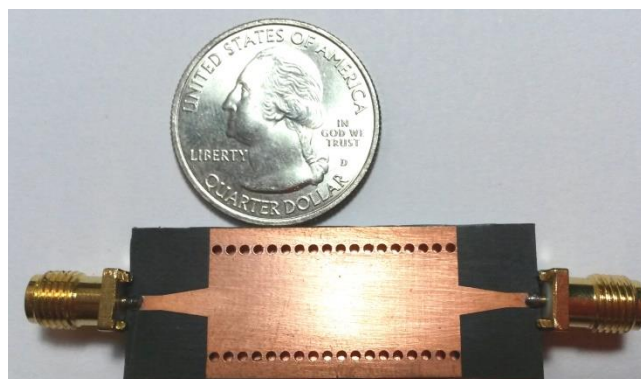


Fig. 7 Structure built to operate in Ku Band.

The measurement setup for the structure operating in Ku Band is shown in Fig. 8.

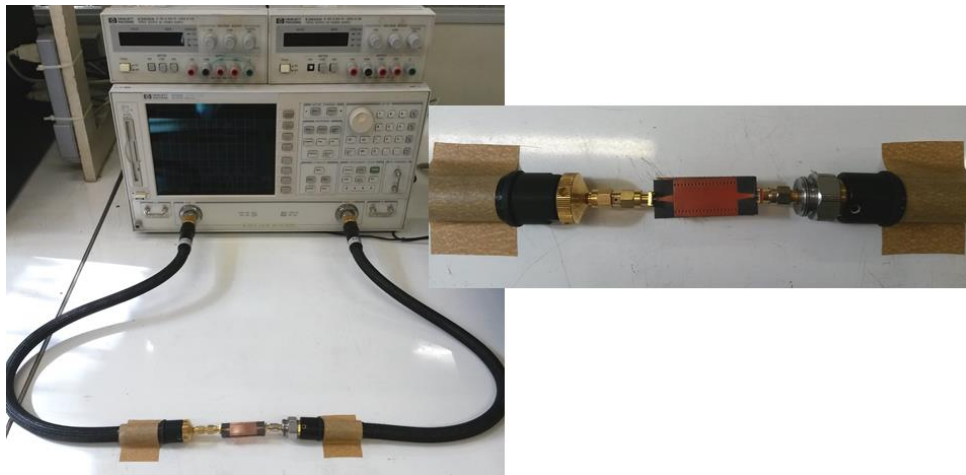


Fig. 8 Structure built to operate in Ku Band.

The simulated and measured S parameters obtained for the structure operating in Ku band are shown in Fig. 9.

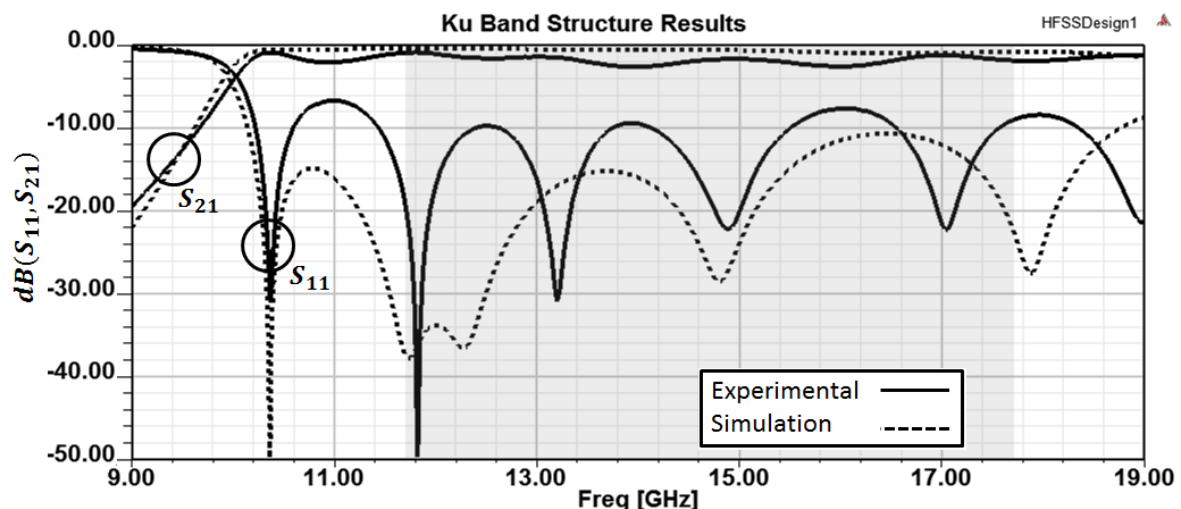


Fig. 9 S parameters obtained for the structure built to operate in Ku Band.

The simulation results indicated return losses better than 10.0 dB in almost the whole recommend bandwidth. The experimental results presented some degradation in comparison with the simulated ones. The calculated value of the reflection coefficient is -17.72 dB, which this match with the experimental results.

V. CONCLUSION

This research work has focused on integration between planar circuits and SIW components. To connect both structures and realize the impedance matching was considered a taper transition. An empirical design procedure based on an approximation according with simulation results and electromagnetic theory was developed to determine the physical dimensions of this particular planar transition.

The proposed approximation in this paper according with simulation results shows an error lower than 6% for the wavelength of an electromagnetic wave being propagated along the taper transition and an error lower than 7% in the impedance matching between the taper transition and the substrate integrated waveguide. The low error obtained allowed the development of two equations to determine the width w_2 and length l_2 of the taper transition.

The designed procedure developed in this paper was applied in two different structures, which the first one operates in X Band and the second one operates in Ku Band. For the structure operating in X Band, the S parameters obtained experimentally shows return loss better than 10.0 dB over 61.67% of the considered bandwidth. The insertion loss is better than 1.90 dB in almost the whole considered bandwidth. For the structure operating in Ku Band, the S parameters obtained experimentally shows return loss better than 10.0 dB over 72.88% of the considered bandwidth. The insertion loss is also better than 1.96 dB in almost the whole considered bandwidth. The proposed design procedure has presented good frequency response. Optimization processes can be realized to improve the final results in the considered structures.

ACKNOWLEDGMENT

The author would like to thank the São Paulo Research Foundation (FAPESP) for the financial support related to research project with process number 2014/10030-7.

REFERENCES

- [1] X. P. Chen, K. Wu, "Substrate Integrated Waveguide Filter," *IEEE Microwave Magazine*, vol. 15, no. 5, pp. 108-116, July-Aug. 2014
- [2] Y. Cassivi, et al, "Dispersion Characteristics of Substrate Integrated Rectangular Waveguides," *IEEE Microwave and Wireless Components Letters*, vol. 12, no. 9, pp. 333-335, Sept. 2002.
- [3] T. Shahvirdi and A. Banai, "Applying Contour Integral Method for Analysis of Substrate Integrated Waveguide Filters," *Microwave Symposium (MMS)-2010 Mediterranean*, 2010, pp. 418- 421.
- [4] D. Deslandes, K. Wu, "Accurate Modeling, Wave Mechanisms, and Design Considerations of a substrate Integrated Waveguide," *IEEE Transactions on Microwave Theory and Techniques*, vol. 54, no. 6, pp. 2516-2526, June 2006.
- [5] F. Xu, K. Wu, "Guided-Wave and Leakage Characteristics of Substrate Integrated Waveguide," *IEEE Transactions on Microwave Theory and Techniques*, vol. 53, no. 6, pp. 66-73, Jan. 2005.
- [6] M. Bozzi, L. Perregrini, K. Wu, "Modeling of Conductor, Dielectric, and Radiation Losses in Substrate Integrated Waveguide by the Boundary Integral-Resonant Mode Expansion Method," *IEEE Transactions on Microwave Theory and Techniques*, vol. 56, no. 12, pp. 3153-3161, Dec. 2008.
- [7] S. Dermain, D. Deslandes, K. Wu, "Development of Substrate Integrated Waveguide Power Dividers," *Canadian Conference on Electrical and Computer Engineering- IEEE CCECE 2003*, 2003, vol.3, pp. 1921-1924.
- [8] C. Wang, W. Che, P. Russer, "High Isolation Multi-way Power Dividing/Combining Network Implemented by Broadside- Coupling SIW Directional Couplers," *International Journal of RF and Microwave Computer*, vol. 19, no. 5, pp. 577-582, Sep. 2009.
- [9] C. Wang, et al, "Multi-way Microwave Planar Power Divider/Combiner Based on Substrate Integrated Rectangular Waveguides Directional Couplers," *International Conference on Microwave and Millimeter Wave technology*, Nanjing, 2008, pp. 18-21.
- [10] D. Deslandes, "Design Equations for Tapered Microstrip-To-Substrate Integrated Waveguide Transitions," *Microwave Symposium Digest (MTT)-2010 IEEE MTT-S International*, 2010, pp. 704-707.
- [11] D. Deslandes, K. Wu, "Integrated Microstrip and Rectangular Waveguide in Planar Form," *IEEE Microwave and Wireless Components Letters*, vol. 11, no. 2, pp. 68-70, Feb. 2001.
- [12] S. Ramo, J. R. Whinnery, T.V. Duzer, "Waveguides With Cylindrical Conducting Boundaries," in *Fields and Waves in Communication Electronics*, 3rd ed., USA: John Wiley & Sons, Inc., 1994, pp. 417-428.
- [13] D. M. Pozar, "Transmissions Lines and Waveguides," in *Microwave Engineering*, 4th ed., USA: John Wiley & Sons, Inc., 2012, pp. 147-153.
- [14] D. M. Pozar, "Impedance Matching and Tuning," in *Microwave Engineering*, 4th ed., USA: John Wiley & Sons, Inc., 2012, pp. 261-267.